International Journal of Heat and Mass Transfer 67 (2013) 581–592

Contents lists available at ScienceDirect

International Journal of Heat and Mass Transfer

journal homepage: www.elsevier.com/locate/ijhmt

An unstructured grids-based discretization method for convection–diffusion equations in the two-dimensional cylindrical coordinate systems

Guojun Yu, Bo Yu *, Yu Zhao, Jingfa Li, Qianqian Shao, Jianyu Xie

National Engineering Laboratory for Pipeline Safety, Beijing Key Laboratory of Urban Oil and Gas Distribution Technology, China University of Petroleum (Beijing), Beijing 102249, China

ARTICLE INFO

Article history:
Received 9 January 2013
Received in revised form 17 May 2013
Accepted 21 August 2013

Keywords:
Cylindrical coordinate
Unstructured grid
Control volume
Discretization method
Finite volume method

ABSTRACT

The study on the application of unstructured grids in the solution of problems in two-dimensional cylindrical coordinate systems (r–z) is scarce, since one of the challenges facing this application is the accurate calculation of the control volumes. In this article, an unstructured grids-based discretization method, in the framework of a finite volume approach, is presented for the solution of the convection–diffusion equations in cylindrical coordinate systems. Numerical simulations are presented for the natural convection and lid-driven cavity flow problems. The numerical results calculated on unstructured grids are found to be in good agreement with those calculated on fine structured meshes. The employment of unstructured grids leads to flexibility of the discretization method for irregular domains of any shape.

1. Introduction

Cylindrical symmetrical problems are usually involved in the calculations of heat transfer and fluid flow. In many cases, due to the symmetry of the computation domain and the solution of the physical problem, the numerical solution of the flow equations could be greatly simplified by expressing both the governing equations and the initial/boundary conditions in a two-dimensional cylindrical coordinate system. Actually, many practical problems could be simplified from three-dimensional ones to two-dimensional ones. There have been many studies on the problems in regular two-dimensional cylindrical coordinate systems, while scarce studies are performed on the irregular ones.

Some previous applications of the two-dimensional cylindrical coordinates to the solution of the three-dimensional cylindrical symmetrical problems are listed below. Bilgili and Ataer [1] investigated the heat and mass transfer for hydrogen absorption in an annular metal hydride bed by a two-dimensional cylindrical coordinate system. Oliveski, Krenzinger et al. [2] analyzed the velocity and temperature fields inside a tank submitted to internal natural and mixed convection using a two-dimensional model in the cylindrical coordinate system through the finite volume method. Yang and Tsai [3] presented a numerical study of transient conjugate heat transfer in a high turbulence air jet impinging over a flat circular disk using a finite volume method in the two-dimensional cylindrical coordinate system. Oliveski and Macagnan et al. [4] investigated the thermal stratification inside a tank containing thermal oil by a two-dimensional model in the cylindrical coordinate system with the finite volumes method. Sievers et al. [5] employed a two-dimensional anisotropic cylindrical coordinate model with linear triangular finite elements to simulate the steady-state temperature distribution within the Li-ion cells.

The computational domains discussed in the previous reports [1–6] are all regular ones, and are all discretized by orthogonal grids. A few reports [7] presented the employment of unstructured grids in two-dimensional cylindrical problems, but their concern was the physical problem in r–θ plane (actually a polar coordinate system), neglecting the gradient in z direction, and thus is different from the issue we concern in the r–z plane. For a r–z cylindrical symmetrical domain shown in Fig. 1(a), as a regular one, it could be mapped by completely orthogonal grids; while for the r–z domain shown in Fig. 1(b), as an irregular one, it could not be mapped by orthogonal grids directly, but could be perfectly mapped by unstructured grids. However, if the unstructured grids are applied in a two-dimensional cylindrical coordinate system (r–z), one challenge is the accurate calculation of the control volume. For structured grids, the calculation of the control volume is easy, i.e. $V_i = r_{P_0}\Delta r_{P_0}\Delta z_{P_0}$, since Δr_{P_0} and Δz_{P_0} are available on a given mesh. But for the unstructured grids in a two-dimensional cylindrical coordinate system, as the grid face is not parallel to

* Corresponding author. Tel.: +86 10 89733849.
E-mail address: yubobox@vip.163.com (B. Yu).

0017-9310/$ - see front matter © 2013 Elsevier Ltd. All rights reserved.
http://dx.doi.org/10.1016/j.ijheatmasstransfer.2013.08.059

Nomenclature

$\boldsymbol{a}$	an arbitrary vector
a_{P0}, a_j	coefficients of the discretized equation
A	bounding surface of a control volume
b	source term
$\mathbf{d}$	direction vector
dA	an infinitesimal surface element
D_j	diffusion term
F_j	mass flux at surface j
g	acceleration due to gravity
Gr	Grashof number
H	height
L	length
L_j	length of the jth boundary segment
$\mathbf{n}$	a unit vector normal to the surface element
p	pressure
Pr	Prandtl number
$\mathbf{r}$	radius vector
r, θ, z	radial, angular and axial coordinate respectively
r_1	inner radius
r_2	outer radius
Re	Reynolds number
S	general source term
T	temperature
$\boldsymbol{U}$	velocity vector
u, v	radial and axial velocity component respectively

Greek symbols

α	thermal diffusivity
β	coefficient of thermal expansion
ΔV_i	control volume of node i
ΔA_j	jth surface element area of a control volume
π	an irrational number, equals 3.14 with two decimal places, dimensionless
ρ	density
ϕ	a general variable
ν	kinematic viscosity
Γ	general diffusion coefficient

Subscripts

c	cool
CV	control volume
h	hot
i	node number
j	surface number of a control volume
P_0	interested node number

Superscripts

$*$	representing dimensionless
n	normal
c	cross

Prefixes

Δ	increment
∇	gradient

the coordinate axes, plus different grid cells are of different shapes and sizes, the calculation of such control volumes is complicated.

To the author's knowledge, the study on the applications of unstructured grids in the solution of convection–diffusion problems in two-dimensional r–z coordinates is not found, and discretization method especially the calculation of the control volume has not been reported. In this article, an unstructured grids-based discretization method, in the framework of a finite volume approach, is proposed for the solution of the convection–diffusion equations in r–z coordinates, and especially an accurate calculation method of the control volumes is presented. After that, the discretization method is validated by three well-designed numerical cases. This study provides some basis for finite volume method.

2. Governing equations and the discretization method

In the two-dimensional cylindrical coordinate system, continuity equation, momentum equation and energy equation of steady state can be described by a general governing equation:

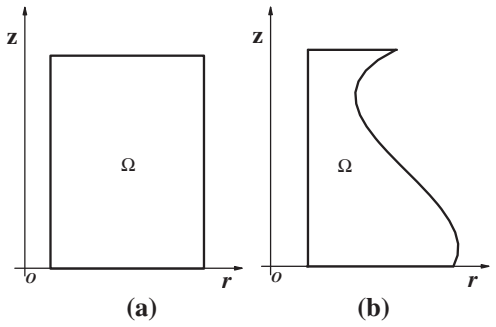

Fig. 1. Two-dimensional regular and irregular cylindrical symmetrical domain: (a) Regular domain (b) Irregular domain.

$$\frac{\partial}{\partial z}(\rho u\phi)+\frac{1}{r}\frac{\partial}{\partial r}(r\rho v\phi)=\frac{\partial}{\partial z}\left(\Gamma\frac{\partial\phi}{\partial z}\right)+\frac{1}{r}\frac{\partial}{\partial r}\left(r\Gamma\frac{\partial\phi}{\partial r}\right)+S \tag{1}$$

where, ϕ is a general variable; Γ and S are the general diffusion coefficient and source term respectively, and details of which for different equation types and physical problems are listed in Table 1. The two terms on the left hand side of the equation are the convection terms; the first two terms on the right hand side are the diffusion terms, and the last term is the general source term. In Table 1, in the source term of the v momentum equation, the underlined part is the buoyancy lift which is treated by a Boussinesq assumption.

The dimensionless equations are derived below taking the examples of natural convection and lid-driven cavity flow problems.

For natural convection, the following dimensionless parameters are defined,

$$r^*=r/L,\quad z^*=z/L,\quad u^*=\frac{\rho L}{\mu}u,\quad v^*=\frac{\rho L}{\mu}v,\quad T^*=\frac{T-T_c}{T_h-T_c},$$

$$p^*=\frac{\rho L^2}{\mu^2}p+\frac{\rho^2 gL^2}{\mu^2}z,\quad \mathrm{Gr}=\rho^2\beta g(T_h-T_c)L^3/\mu^2$$

Table 1
Coefficients and source terms of the governing equation for lid-driven cavity and natural convection problem.

Equation	ϕ	Γ^*	S	
			Lid-driven cavity	Natural convection
Continuity equation	1	0	0	0
Momentum equation	u	μ	$-\frac{\partial p}{\partial r}-\frac{\mu u}{r^2}$	$-\frac{\partial p}{\partial r}-\frac{\mu u}{r^2}$
	v	μ	$-\frac{\partial p}{\partial z}$	$-\frac{\partial p}{\partial z}+\underline{\rho g\beta(T-T_c)}$
Energy equation	T	$\frac{\mu}{\mathrm{Pr}}$	–	0

Subsequently, the dimensionless governing equations of the natural convection problem are written as follows:

$$\frac{\partial(u^*u^*)}{\partial z^*}+\frac{1}{r^*}\frac{\partial(r^*v^*u^*)}{\partial r^*}=-\frac{\partial p^*}{\partial z^*}+\frac{\partial}{\partial z^*}\left(\frac{\partial u^*}{\partial z^*}\right)+\frac{1}{r^*}\frac{\partial}{\partial r^*}\left(r^*\frac{\partial u^*}{\partial r^*}\right)-\frac{u^*}{r^{*2}} \tag{2}$$

$$\frac{\partial(u^*v^*)}{\partial z^*}+\frac{1}{r^*}\frac{\partial(r^*v^*v^*)}{\partial r^*}=-\frac{\partial p^*}{\partial r^*}+\frac{\partial}{\partial z^*}\left(\frac{\partial v^*}{\partial z^*}\right)+\frac{1}{r^*}\frac{\partial}{\partial r^*}\left(r^*\frac{\partial v^*}{\partial r^*}\right)+\mathrm{Gr}T^* \tag{3}$$

$$\frac{\partial(u^*T^*)}{\partial z^*}+\frac{1}{r^*}\frac{\partial(r^*v^*T^*)}{\partial r^*}=\frac{1}{\mathrm{Pr}}\frac{\partial}{\partial z^*}\left(\frac{\partial T^*}{\partial z^*}\right)+\frac{1}{\mathrm{Pr}}\frac{1}{r^*}\frac{\partial}{\partial r^*}\left(r^*\frac{\partial T^*}{\partial r^*}\right) \tag{4}$$

For lid-driven cavity flow problem, the following dimensionless parameters are defined.

$$u^*=u/u_{top},\quad v^*=v/u_{top},\quad z^*=z/L,\quad r^*=r/L,$$
$$p^*=p/\rho u_{top}^2,\quad \mathrm{Re}=\frac{\rho u_{top}L}{\mu}$$

Thus the dimensionless governing equations of lid-driven cavity flow problem are as follows:

$$\frac{\partial(u^*u^*)}{\partial z^*}+\frac{1}{r^*}\frac{\partial(r^*v^*u^*)}{\partial r^*}=-\frac{\partial p^*}{\partial z^*}+\frac{1}{\mathrm{Re}}\frac{\partial}{\partial z^*}\left(\frac{\partial u^*}{\partial z^*}\right)+\frac{1}{\mathrm{Re}}\frac{1}{r^*}\times\frac{\partial}{\partial r^*}\left(r^*\frac{\partial u^*}{\partial r^*}\right)-\frac{1}{\mathrm{Re}}\frac{u^*}{r^{*2}} \tag{5}$$

$$\frac{\partial(u^*v^*)}{\partial z^*}+\frac{1}{r^*}\frac{\partial(r^*v^*v^*)}{\partial r^*}=-\frac{\partial p^*}{\partial z^*}+\frac{1}{\mathrm{Re}}\frac{\partial}{\partial z^*}\left(\frac{\partial v^*}{\partial z^*}\right)+\frac{1}{\mathrm{Re}}\frac{1}{r^*}\times\frac{\partial}{\partial r^*}\left(r^*\frac{\partial v^*}{\partial r^*}\right) \tag{6}$$

2.1. An unstructured grids-based finite volume discretization method

On unstructured grids, the steady-state dimensionless convection–diffusion equation in a tensor form is given by Eq. (7). For different physical problems and equation types, such as the natural convection problem and lid-driven cavity problem, the coefficients and source terms are listed in Table 2.

$$div(\mathbf{U}^*\phi^*)-div(\Gamma^*grad\phi^*)=S^* \tag{7}$$

where $\mathbf{U}$ represents the velocity vector, $\mathbf{U}=ui+vj$.

Integrating Eq. (7) over the control volume CV gives:

$$\int_{CV}div(\mathbf{U}^*\phi^*)dV^*-\int_{CV}div(\Gamma^*grad\phi^*)dV^*=\int_{CV}S^*dV^* \tag{8}$$

Here we introduce Gauss theorem shown as in Eq. (9), which is applicable to any shape of control volume.

$$\int_{CV}div\,\mathbf{a}\,dV=\int_A\mathbf{n}\cdot\mathbf{a}\,dA \tag{9}$$

Table 2
Coefficients and source terms of the dimensionless governing equation for natural convection and lid-driven cavity problem.

Equation type	ϕ^*	Γ^*		S^*	
		Natural convection	Lid-driven cavity flow	Natural convection	Lid-driven cavity flow
Continuity equation	1	0	1	0	0
Momentum equation	u^*	1	$\frac{1}{\mathrm{Re}}$	$-\frac{\partial p^*}{\partial r^*}-\frac{u^*}{r^{*2}}$	$-\frac{\partial p^*}{\partial r^*}-\frac{1}{\mathrm{Re}}\frac{u^*}{r^{*2}}$
	v^*	1	$\frac{1}{\mathrm{Re}}$	$-\frac{\partial p^*}{\partial z^*}+\mathrm{Gr}T^*$	0
Energy equation	T^*	$\frac{1}{\mathrm{Pr}}$	–	0	–

where $\boldsymbol{a}$ is an arbitrary vector, and $\mathbf{n}$ is the unit vector normal to infinitesimal surface element dA.

Application of Gauss theorem to Eq. (8) gives

$$\int_A\mathbf{n}\cdot(\mathbf{U}^*\phi^*)dA^*-\int_A\mathbf{n}\cdot(\Gamma^*grad\phi^*)dA^*=\int_{CV}S^*_{P_0}dV^* \tag{10}$$

The area integrations are carried out over all surface segments, so Eq. (10) can be written as follows:

$$\sum_{all\ surfaces}\int_{\Delta A_j}\mathbf{n}_j\cdot(\mathbf{U}^*\phi^*)dA^*-\sum_{all\ surfaces}\int_{\Delta A_j}\mathbf{n}_j\cdot(\Gamma^*grad\phi^*)dA^*=\int_{CV}S^*_{P_0}dV^* \tag{11}$$

where ΔA_j represents the jth surface element area.

The first term on the left hand side is discretized as follows:

$$\sum_{all\ surfaces}\int_{\Delta A_j}\mathbf{n}_j\cdot(\mathbf{U}^*\phi^*)dA^*=\sum_{all\ surfaces}F_j\phi^*_j \tag{12}$$

where $F_j=\mathbf{n}_j\cdot(\mathbf{U}^*\phi^*)\Delta A^*_j$.And the second term on the left hand side is discretized as follows:

$$D_j=-\int_{\Delta A_i}\mathbf{n}_j\cdot(\Gamma^*grad\phi^*)dA^*=-\mathbf{n}_j\cdot(\Gamma^*grad\phi^*)\Delta A^*_j \tag{13}$$

D_j is divided into two components, a normal component and a cross-diffusion component:

$$D_j=D^n_j+D^c_j \tag{14}$$

where

$$D^n_j=\mathbf{n}_j\cdot\left(\frac{\phi^*_{P_j}-\phi^*_{P_0}}{\left|\mathbf{d}^*_j\right|}\frac{\mathbf{d}^*_j}{\left|\mathbf{d}^*_j\right|}\right)\Gamma^*_j\Delta A^*_j \tag{15}$$

$$D^c_j=\mathbf{n}_j\cdot\left(\nabla\phi^*_j-\nabla\phi^*_j\cdot\frac{\mathbf{d}^*_j}{\left|\mathbf{d}^*_j\right|}\cdot\frac{\mathbf{d}^*_j}{\left|\mathbf{d}^*_j\right|}\right)\Gamma^*_j\Delta A^*_j \tag{16}$$

The gradient on the surface j is determined by

$$\nabla\phi^*_{P_j}=\nabla\phi^*_{P_0}\frac{\left|\mathbf{r}^*_j-\mathbf{r}^*_{P_j}\right|}{\left|\mathbf{d}^*_j\right|}+\nabla\phi^*_{P_j}\frac{\left|\mathbf{r}^*_{P_0}-\mathbf{r}^*_j\right|}{\left|\mathbf{d}^*_j\right|} \tag{17}$$

The source term is discretized as

$$\int_{CV}S^*_{P_0}dV=S^*_{P_0}\Delta V^*_{P_0} \tag{18}$$

where $\Delta V^*_{P_0}$ is the control volume of node P_0.

For the unstructured triangular grids, substituting Eqs. (12)–(18) into Eq. (11) gives

$$\sum_{j=1}^{3}F_j\phi^*_j-\sum_{j=1}^{3}\mathbf{n}_j\cdot\left(\frac{\phi^*_{P_j}-\phi^*_{P_0}}{\left|\mathbf{d}^*_j\right|}\frac{\mathbf{d}^*_j}{\left|\mathbf{d}^*_j\right|}\right)\Gamma^*_j\Delta A^*_j-\sum_{j=1}^{3}\mathbf{n}_j\cdot\left(\nabla\phi^*_j-\nabla\phi^*_j\cdot\frac{\mathbf{d}^*_j}{\left|\mathbf{d}^*_j\right|}\cdot\frac{\mathbf{d}^*_j}{\left|\mathbf{d}^*_j\right|}\right)\Gamma^*_j\Delta A^*_j=S^*_{P_0}\Delta V^*_{P_0} \tag{19}$$

In Eq. (19),

$$\phi^*_j=\max(F_j,0)\left[\phi^*_{P_0}+(\nabla\phi^*)_j\cdot\left(\mathbf{r}^*_j-\mathbf{r}^*_{P_0}\right)\right]-\max(-F_j,0)\left[\phi^*_{P_j}+(\nabla\phi^*)_j\cdot(\mathbf{r}^*_j-\mathbf{r}^*_{P_j})\right] \tag{20}$$

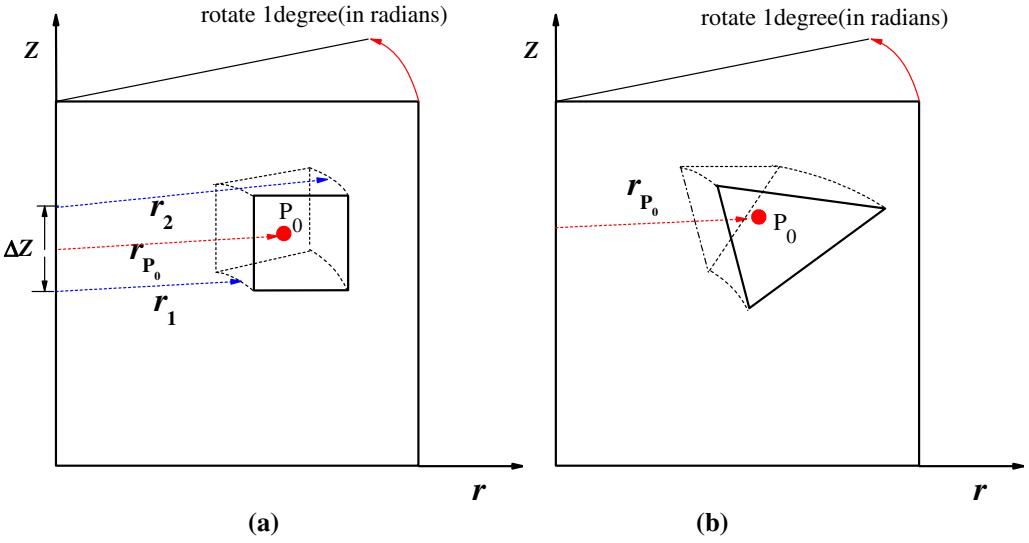

Fig. 2. Sketch map of structured and unstructured control volumes in a two-dimensional cylindrical coordinate system: (a) Structured, (b) Unstructured.

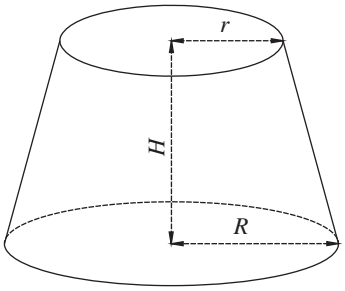

Fig. 3. C truncated cone formed by rotating a right trapezoid by 360 degrees.

So, the discretized equation is obtained as follows:

$$a_{P_0}\phi^*_{P_0} = \sum_{j=1}^{3} a_j \phi^*_j + b \tag{21}$$

where

$$a_j = \mathbf{n}_j \cdot \frac{\mathbf{d}^*_j}{|\mathbf{d}^*_j|^2}\Gamma^*_j \Delta A^*_j + (\max(F_j, 0) - F_j) \tag{22}$$

$$a_{P_0} = \sum_{i=1}^{3} a_j - S^*_{P_0}\phi^*_{P_0} \tag{23}$$

$$b = \sum_{j=1}^{3}\Big(-\max(F_j,0)(\nabla\phi^*)_j \cdot (\mathbf{r}^*_j - \mathbf{r}^*_{P_0}) + \max(-F_j,0)(\nabla\phi^*)_j \cdot (\mathbf{r}^*_j - \mathbf{r}^*_{P_j}) + \mathbf{n}_j \cdot \left(\nabla\phi^*_j - \nabla\phi^*_j \cdot \frac{\mathbf{d}^*_j}{|\mathbf{d}^*_j|} \cdot \frac{\mathbf{d}^*_j}{|\mathbf{d}^*_j|}\right)\Gamma^*_j \Delta A^*_j + S^*_{P_0}\Delta V^*_{P_0}\Big) + S^*_{P_0}\Delta V^*_{P_0} \tag{24}$$

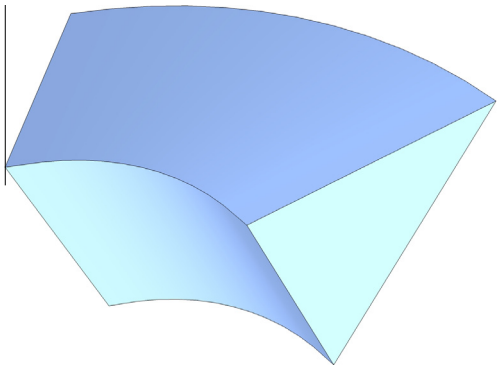

Fig. 5. The stereogram of the triangular control volume (situation 1).

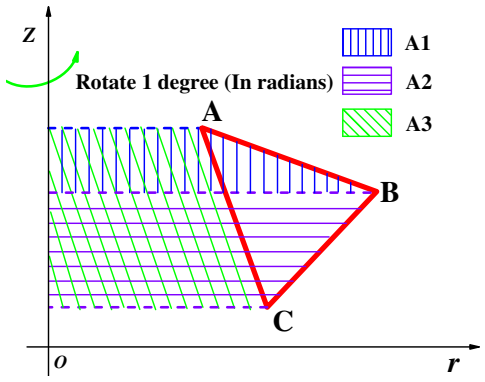

Fig. 4. Combination and split method to determine the control volume (situation 1).

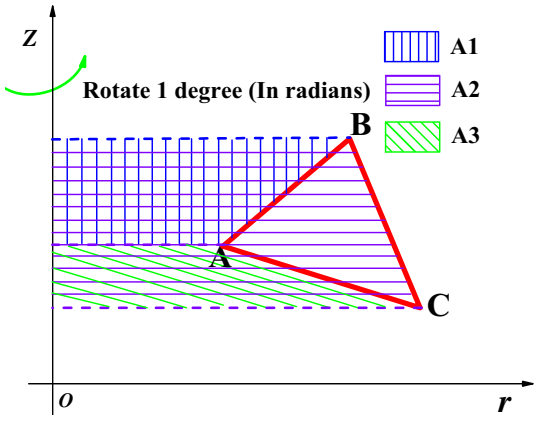

Fig. 6. Combination and split method to determine the control volume (situation 2).

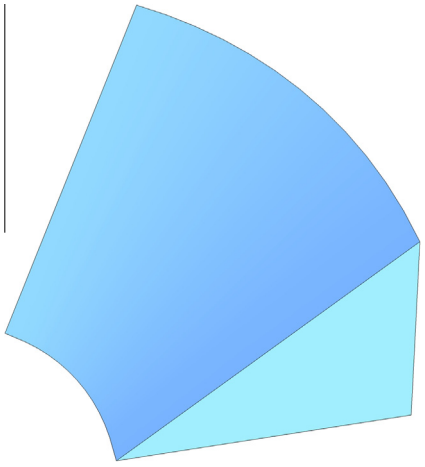

Fig. 7. The stereogram of the triangular control volume (situation 2).

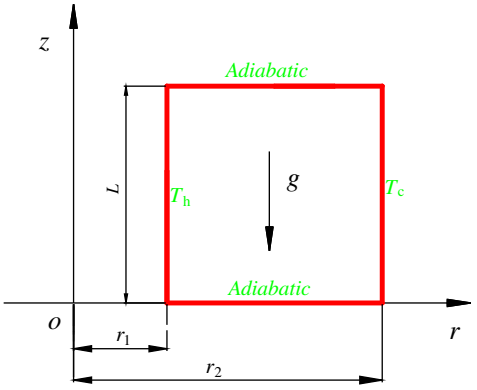

Fig. 8. Computation domain and boundary condition for the two-dimensional cylindrical coordinate natural convection problem.

Eqs. (21)–(24) are applicable to any coordinate systems with different calculations of surface element area ΔA_j and control volume ΔV_{P_0}. Taking structured mesh as an example, in a two-dimensional Cartesian coordinate system, $\Delta A_j = \Delta r_{P_0}$ (the surface parallel to the r axis) or $\Delta A_j = \Delta z_{P_0}$ (the face parallel to the z axis) and the control volume can be determined by $\Delta V_{P_0} = \Delta r_{P_0} \Delta z_{P_0}$; while in a two-dimensional cylindrical coordinate system, face vector $\Delta A_j = r_j \Delta z_{P_0}$ (the left and right faces) or $\Delta A_j = r_{P_0} \Delta r_{P_0}$ (the upper and lower faces) and the control volume can be calculated by $\Delta V_{P_0} = r_{P_0} \Delta r_{P_0} \Delta z_{P_0}$ (shown in Fig. 2(a)). For unstructured grids in a two-dimensional cylindrical coordinate system, the calculation of each face factor is also easy to perform, i.e. $\Delta A_j = r_j L_j$ (here r_j is the r coordinate of the midpoint at jth boundary segment, and L_j is the length of the jth boundary segment), but the calculation of control volume is complicated since the control volume is an irregular pentahedron as sketched in Fig. 2(b), of which the size and shape are dependent on the relative position of the three vertexes. The calculation of the control volume could not be determined by the same procedures as structured grids' and require complicated procedures which will be proposed in the following section.

Table 3
Computation parameters in Example 1.

Case number	r_1^*	r_1^*/r_2^*	Gr
1	0.01	0.0099	10^5
2	0.01	0.0099	10^6
3	0.1	0.0909	10^5
4	0.1	0.0909	10^6
5	1.0	0.5000	10^5
6	1.0	0.5000	10^6

2.2. An accurate calculation method of unstructured control volumes in a two-dimensional cylindrical coordinate system

As discussed above, the calculation of the unstructured control volume V_{P_0} in a two-dimensional cylindrical coordinate system is a challenge. And in this section, an accurate calculation method of unstructured control volume is proposed.

It is known that, a solid of revolution formed by rotating a right trapezoid by 360 degrees is a circular truncated cone as shown in Fig. 3, the volume of which is easy to calculate by:

$$V = \frac{\pi}{3} H(R^2 + r^2 + Rr) \tag{25}$$

A right trapezoid can be constructed by each edge of the triangular cell, two lines parallel to r-axis, plus z-axis. The right trapezoids involving edges AB, BC and AC are named A_1, A_2 and A_3 respectively, and an example could be found in Fig. 4. Since the area of the

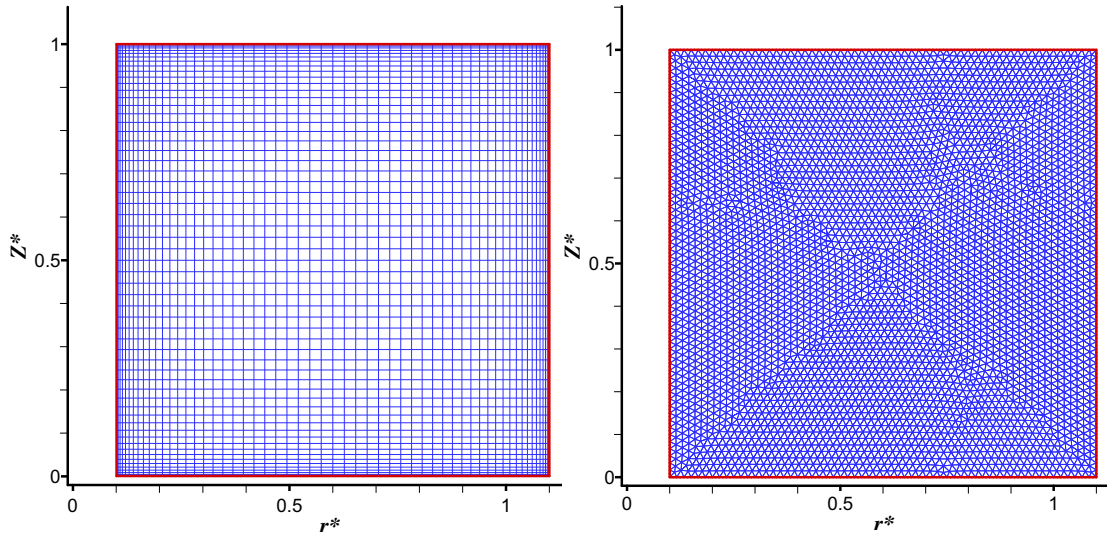

Fig. 9. Grid system (coarse).

triangular cell is the algebraic sum of A_1, A_2 and A_3, the solid of revolution by rotating the triangle ABC about z-axis by 360 degrees could be determined by the combination of three circular truncated cones formed by rotating A_1, A_2 and A_3.

Define vertex A is the one with the smallest r, B is the one with the greater z between the others two points and C is the remaining one. Due to the different relative positions of the three vertexes of a triangular cell, combination of A_1, A_2 and A_3 may be different. Based on the above assumptions, there are 6 different relative positions of the three vertexes of a triangle, i.e. ($z_1 < z_3 < z_2$ and $r_2 < r_3$), ($z_1 < z_3 < z_2$ and $r_2 > r_3$), ($z_3 < z_2 < z_1$ and $r_2 < r_3$), ($z_3 < z_2 < z_1$ and $r_2 > r_3$), ($z_3 < z_1 < z_2$ and $r_2 < r_3$) and ($z_3 < z_1 < z_2$ and $r_2 > r_3$). If $z_1 < z_3 < z_2$ or $z_3 < z_2 < z_1$, the area of triangular ABC is $S_{\Delta ABC} = A_1 + A_2 - A_3$ regardless of r. If $z_3 < z_1 < z_2$, the area of

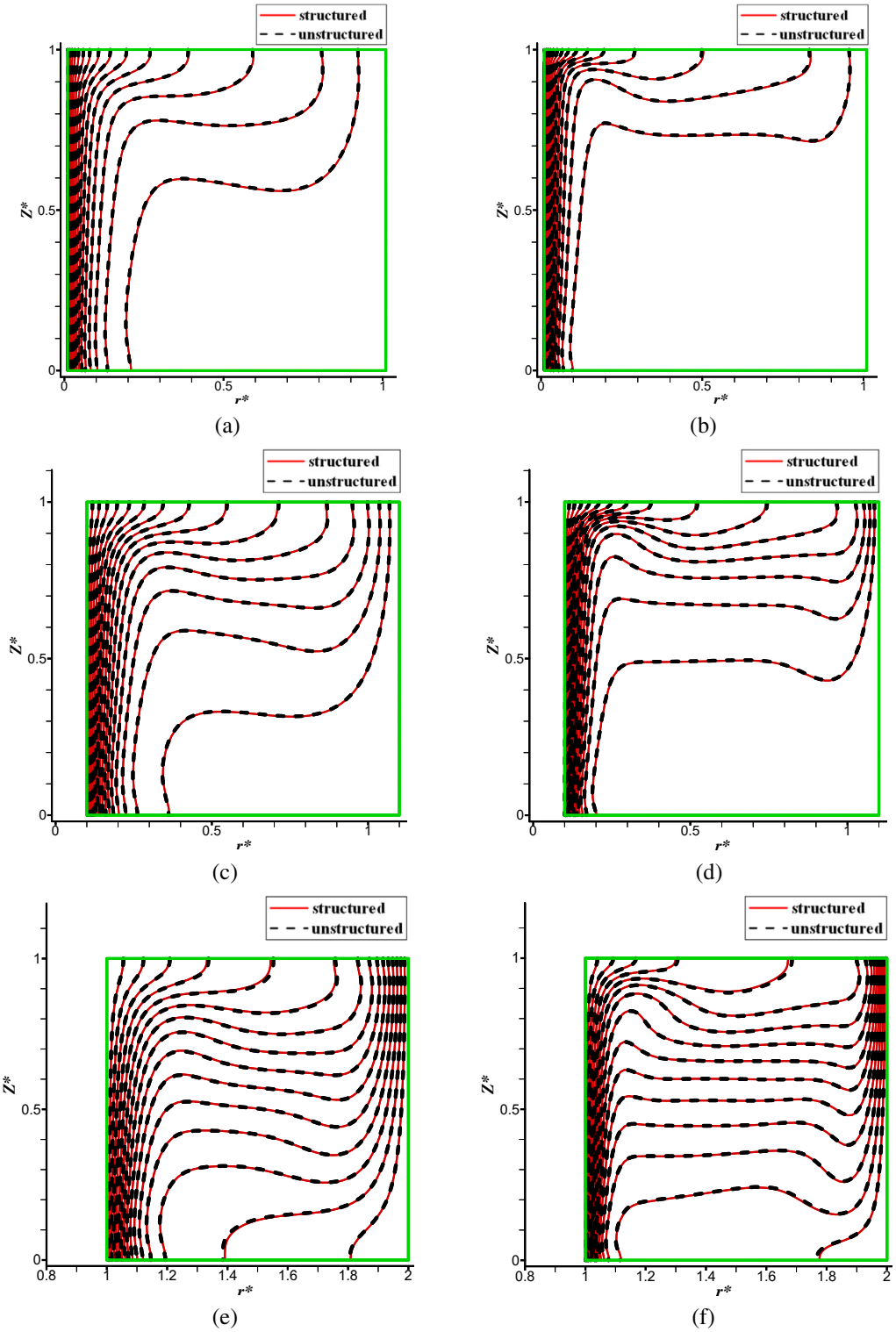

Fig. 10. Comparison of temperature fields for the natural convection in Example 1.

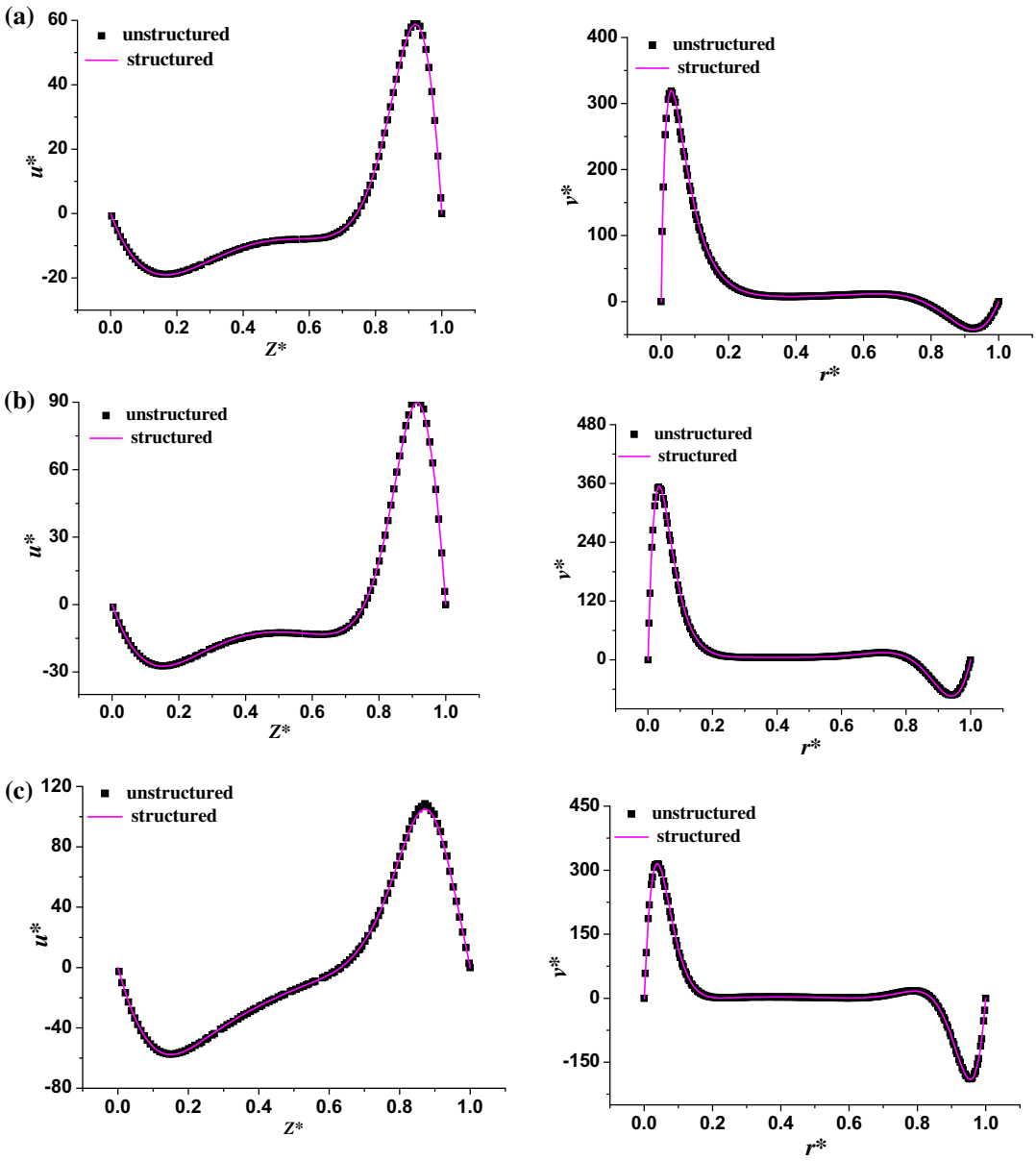

Fig. 11. Comparison of centerline velocity components for the natural convection in Example 1.

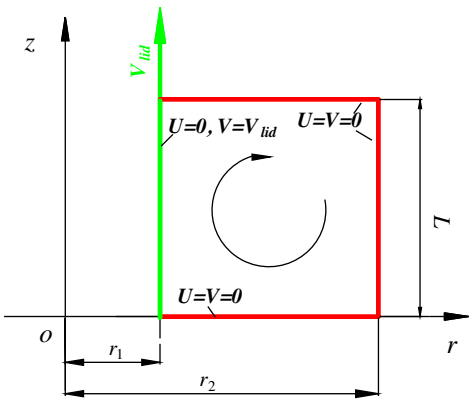

Fig. 12. Computation domain and boundary conditions for the cylindrical square cavity lid-driven cavity problem.

Table 4
Computation parameters in Example 2.

Case number	r_1^*	r_1^*/r_2^*	Re
1	0.01	0.0099	10^3
2	0.1	0.0909	10^3
3	1.0	0.5000	10^3

triangular ABC is $S_{\Delta ABC} = A_2 - A_1 - A_3$ regardless of r. So, there are only two situations in total, i.e. $z_1 < z_3 < z_2$ or $z_3 < z_2 < z_1$ (situation 1), and $z_3 < z_1 < z_2$ (situation 2).

For situation 1, taking $r_2 > r_3$ as an example, the combination and split method to determine the control volume is shown in Fig. 4.

Define V_1, V_2 and V_3 are the volumes of the circular truncated cones formed by A_1, A_2 and A_3, and the coordinates of the vertexes A, B and C are respectively (r_1, z_1), (r_2, z_2) and (r_3, z_3).

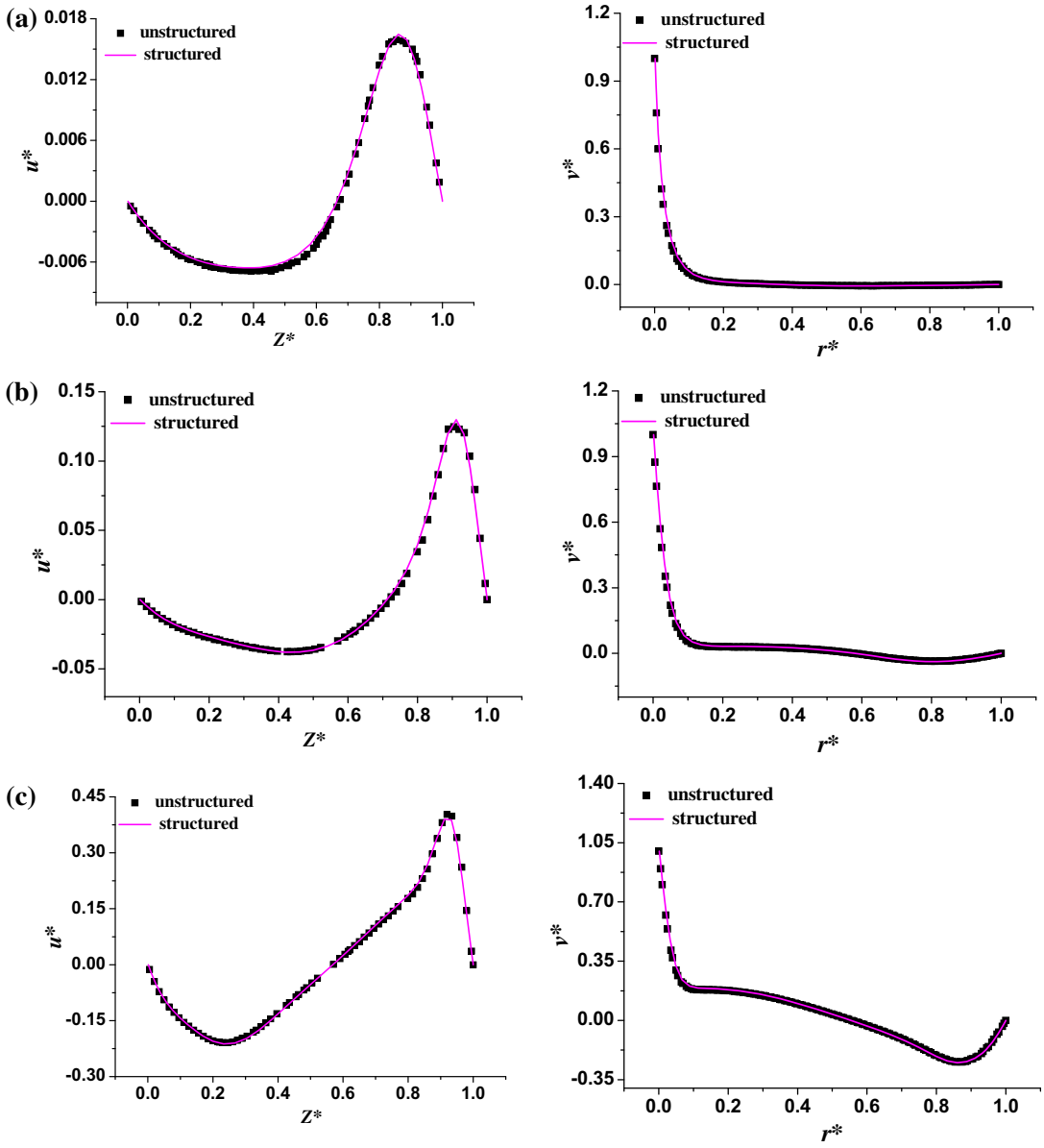

Fig. 13. Comparison of centerline velocity components for the lid-driven cavity problem.

So V_1, V_2 and V_3 can be calculated by Eq. (25), giving

$$V_1 = \frac{\pi}{3}(z_1 - z_2)(r_1^2 + r_2^2 + r_1 r_2)$$
$$V_2 = \frac{\pi}{3}(z_2 - z_3)(r_2^2 + r_3^2 + r_2 r_3)$$
$$V_3 = \frac{\pi}{3}(z_1 - z_3)(r_1^2 + r_3^2 + r_1 r_3)$$

Since $S_{\Delta ABC} = A_1 + A_2 - A_3$, the control volume of the solid of revolution formed by rotating triangle ABC by 360 degrees can be calculated by

$$\begin{aligned} V_{ABC} &= V_1 + V_2 - V_3 \\ &= \frac{\pi}{3} \times [(z_1 - z_2)(r_1^2 + r_2^2 + r_1 r_2) + (z_2 - z_3)(r_2^2 + r_3^2 + r_2 r_3) \\ &\quad - (z_1 - z_3)(r_1^2 + r_3^2 + r_1 r_3)] \end{aligned}$$

According to the fundamental of two-dimensional cylindrical coordinate system, the control volume of triangle ABC should be

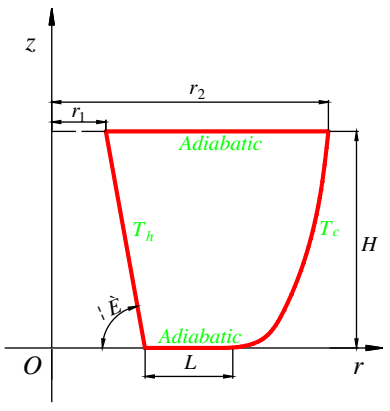

Fig. 14. Computational domain and boundary conditions.

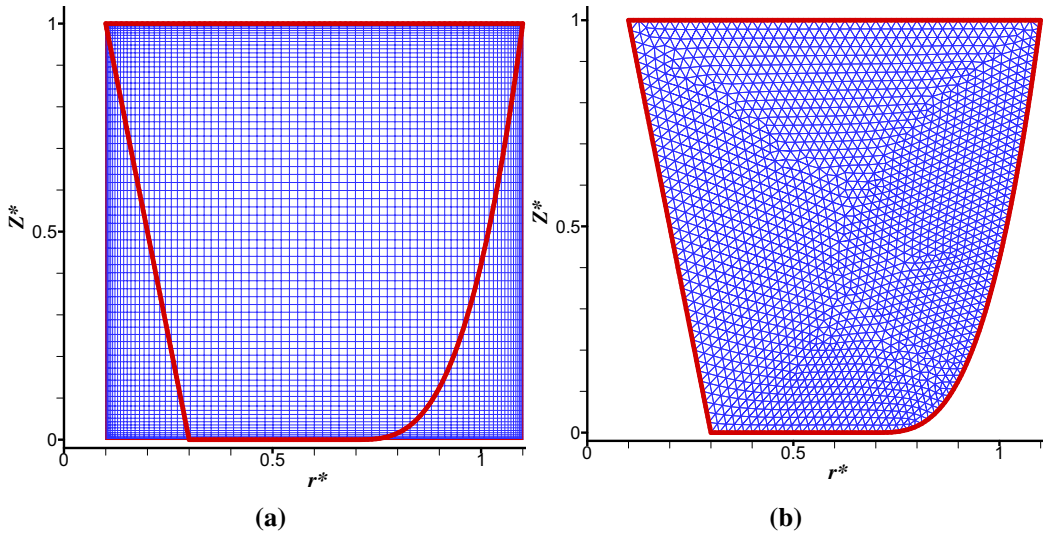

Fig. 15. The grid system in Example 3: (a) Structured; (b) Unstructured.

the volume of the solid of revolution formed by rotating the triangle ABC by 1 degree, shown in Fig. 5. Hence

$$V_{CV} = \frac{V_{ABC}}{2\pi} = \frac{1}{6}\times[(z_1-z_2)(r_1^2+r_2^2+r_1r_2)+(z_2-z_3)(r_2^2+r_3^2+r_2r_3) - (z_1-z_3)(r_1^2+r_3^2+r_1r_3)]$$

For situation 2, taking $r_2 < r_3$ for example, the combination and split method is shown in Fig. 6. V_1, V_2 and V_3 can be defined and expressed similar with situation 1. According Fig. 6, we have,$S_{\Delta ABC} = A_2 - A_1 - A_3$.Hence,

$$V_{ABC} = V_2 - V_1 - V_3 = \frac{\pi}{3}\times[(z_2-z_3)(r_2^2+r_3^2+r_2r_3)-(z_2-z_1)(r_1^2+r_2^2+r_1r_2) - (z_1-z_3)(r_1^2+r_3^2+r_1r_3)]$$

It is deduced that,

$$V_{CV} = \frac{V_{ABC}}{2\pi} = \frac{1}{6}\times\left[(z_2-z_3)(r_2^2+r_3^2+r_2r_3) -(z_2-z_1)(r_1^2+r_2^2+r_1r_2)-(z_1-z_3)(r_1^2+r_3^2+r_1r_3)\right]$$

The stereogram of the triangular control volume is shown in Fig. 7.

The unstructured control volume could be determined conveniently by the above mentioned combination and split methods. Although the method is performed on the triangular grids, same procedures could be straightforwardly extended to that on an unstructured quadrilateral grids system.

3. Numerical examples and results discussions

Three numerical examples, named Example 1, Example 2 and Example 3, are well devised to verify the correctness of the proposed unstructured grids-based discretization method. Example 1 and Example 2 are associated with the two-dimensional natural convection problem and lid-driven cavity flow problem within a regular computation domain in a cylindrical coordinate system respectively, while Example 3 is that in an irregular domain.

Since the structured grids-based discretization method for the two-dimensional convection–diffusion equation in a cylindrical coordinate is mature, and can be found in some literatures, and the results can be validated by some benchmark solutions as well, we choose the results on structured grids as the reference solution to validate the results on unstructured grids. In addition, the results for Example 3 (irregular domain) will also be validated by the results calculate by FLUENT.

In Example 1, the natural convection problem in a cylindrical cavity is concerned. Due to the symmetry, the physical problem could be reduced to a two-dimensional coordinate one. The computation domain and boundary conditions are shown in Fig. 8, in which r_1 and $r_1 + L$ indicate the inner diameter and outer diameter respectively, where L is the length of each boundary. The left and right boundaries are of the first-type boundary conditions, with higher temperature of T_h on the left boundary (inner cylinder wall) and cooler temperature of T_c on the right one (outer cylinder wall) and insulated boundary condition for the upper and lower boundaries. Other parameters are listed in Table 3.

The computation domains are mapped by structured and unstructured grids respectively, which are shown in Fig. 9. In this example, the validations of the proposed method are performed with five cases with different computation parameters shown in Table 3. In the table, $r_1^* = r_1/L$, $r_2^* = r_2/L$.

With the six groups of computation parameters as listed in Table 3, the natural convection problem is calculated by both the structured grids-based method and unstructured grids-based method. The numerical results calculated by the two approaches are compared. Fig. 10 presents the comparison of temperature fields calculated by the two methods, of which the results agree well with each other. It can also be found that with the increase of r_1^*/r_2^*, the temperature fields are gradually approaching to the benchmark solution [7] of a Cartesian coordinate case with same computation parameters. In addition, Fig. 11 presents the comparison of the centerline velocity components calculated by the two methods, also showing good agreement between them. All the

Table 5
Computation parameters in Example 3.

Case number	r_1^*	r_1^*/r_2^*	Gr
1	0.01	0.0099	10^5
2	0.01	0.0099	10^6
3	0.1	0.0909	10^5
4	0.1	0.0909	10^6
5	1.0	0.5	10^5
6	1.0	0.5	10^6

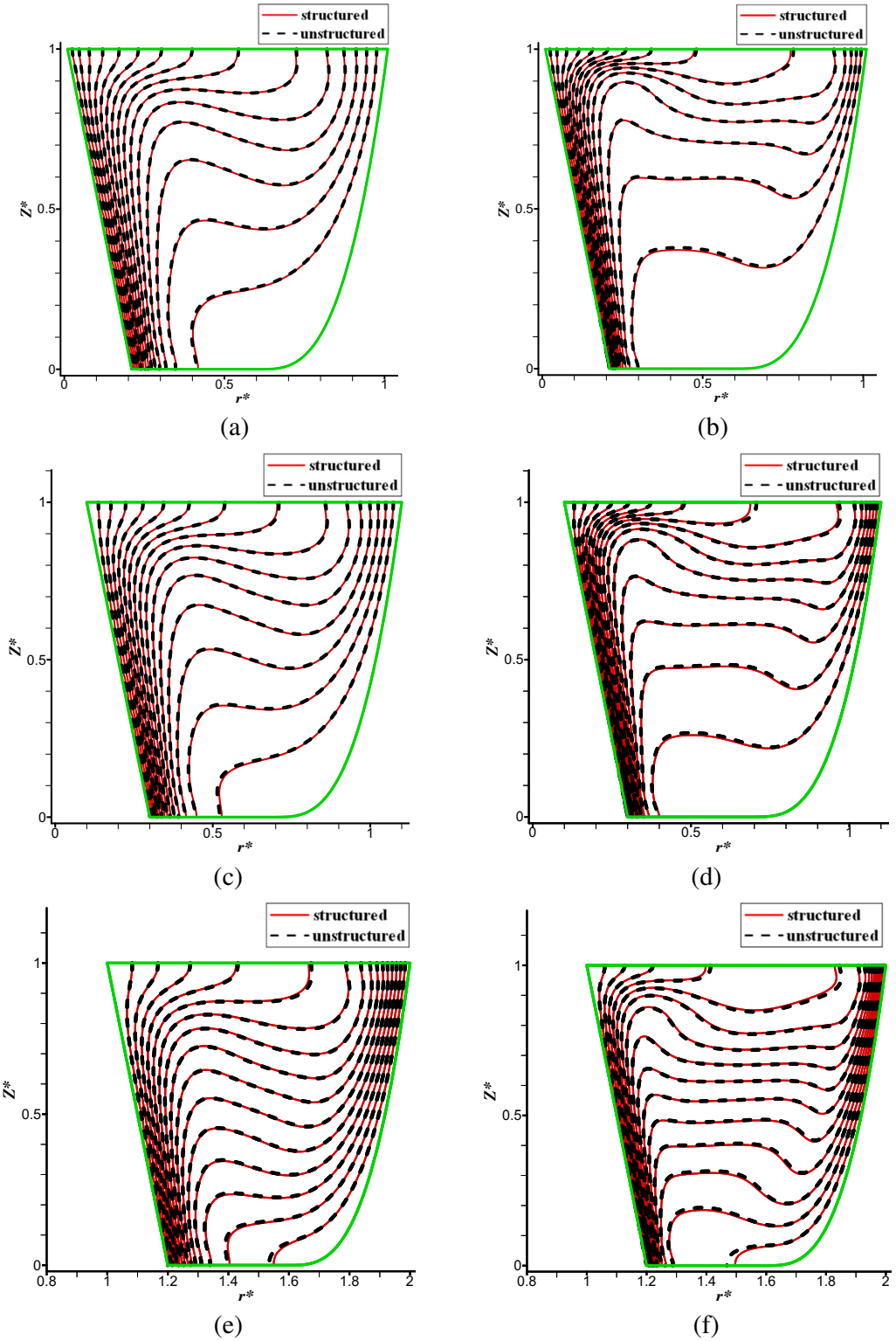

Fig. 16. Comparison of temperature fields with different computation parameters: (a) $r_1^* = 0.01, \mathrm{Gr} = 10^5$; (b) $r_1^* = 0.01, \mathrm{Gr} = 10^6$; (c) $r_1^* = 0.1, \mathrm{Gr} = 10^5$; (d) $r_1^* = 0.1, \mathrm{Gr} = 10^6$; (e) $r_1^* = 1.00, \mathrm{Gr} = 10^5$; (f) $r_1^* = 1.00, \mathrm{Gr} = 10^6$.

numerical results indicate that the proposed unstructured grids-based discretization method is reasonable and accurate.

In Example 2, a lid-driven cavity flow problem in a cylindrical cavity is investigated by a two-dimensional cylindrical coordinate model. The computation domain and boundary conditions are sketched in Fig. 12, in which r_1 and r_2 indicate the inner diameter and outer diameter. The length of each boundary is L. A constant velocity is persistently applied on the left boundary (inner cylinder wall). Other parameters are listed in Table 4. In the table, $r_1^* = r_1/L$, $r_2^* = r_2/L$.

The flow fields of the lid-driven cavity flow are calculated by the structured grids-based method and unstructured grids-based

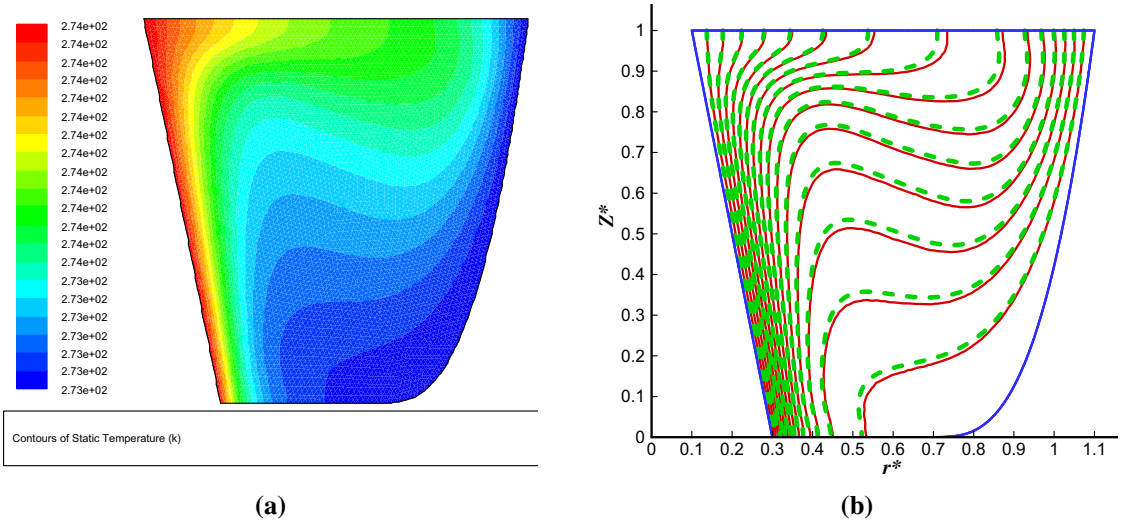

(a) **(b)**

Fig. 17. Comparison of temperature fields calculated by the proposed method and those calculated by fluent at $r_1^* = 0.1$, $\mathrm{Gr} = 10^5$: (a) contours of temperature field calculated by FLUENT; (b) comparison of temperature fields calculated by the proposed method and FLUENT.

method respectively with the parameters listed in Table 4, and the centerline velocity component are compared in Fig. 13. It can be seen that the results of the two methods agree well with each other, and with the increase of r_1^*/r_2^*, the results are gradually approaching to the benchmark solution [8] of a Cartesian coordinate case with identical computation parameters, which indicates the proposed unstructured grids-based method is accurate.

The computation domain involved in the two above-referred examples are all regular and could be mapped by the structured grids, and the advantage and irreplaceability of unstructured grids in a two-dimensional cylindrical coordinate are not revealed. So, in Example 3, the natural convection in an irregular cylindrical cavity is investigated. The three-dimensional cavity is a solid of revolution formed by rotating the geometry shape shown in Fig. 14 about z-axis by 360 degrees. Due to the symmetry of the physical domain and solutions, only the two-dimension domain shown in Fig. 14 needs to be investigated. In the figure, the length of the upper boundary is $r_2 - r_1 = H = 1$ m, and the length of the lower boundary $L = 0.4$ m. The right curve boundary is determined by a cubic curve defined as $z = \frac{1}{0.4^3}[r - (r_1 + 0.6)]^3$. The left and right boundaries are of the first-type boundary conditions, with higher temperature of T_h at the left boundary and cooler temperature of T_c on the right one and insulated boundary condition for the upper and lower boundaries.

For the irregular domain shown in Fig. 14, it is impossible to map it with orthogonal structured grids, but it can be mapped perfectly by the unstructured grid such as triangular grids. To validate the correctness of the proposed method the irregular domain is involved in a square domain shown in Fig. 15(a), and this square domain could be mapped by orthogonal structured grids. Under this circumstance, the boundary condition is affected on the nodes which are adjacent to the real boundary, i.e. the first-type boundary condition can be given to the left boundary and right boundary by assigning all the grid nodes in the lower left region of the left boundary and the lower right region of the right boundary with the values corresponding to the real boundary conditions respectively. If the grids are dense enough, the grid approximated method is acceptable. Fig. 15 presents the structured and unstructured grid systems (a coarse one) for the irregular domain in Example 3. A group of results are calculated on a structured grid system with dense enough cells, and chosen to be the reference solutions. The results calculated by the unstructured grids are compared with these reference solutions to validate the correctness. In addition, the results calculated by FLUENT software are also employed to validate the results calculated by the proposed method. With the computation parameters as shown in Table 5, the temperature fields are calculated by the two methods and compared. In Table 5, $r_1^* = r_1/H$, $r_2^* = r_2/H$.

Fig. 16 presents the comparison of temperature fields calculated by the structured grids-based and the unstructured grids-based discretization method, with the computation parameters as listed in Table 5. It can be seen that the results of the two methods agree well with each other. With structured grids, large amount of grid cells are required to approximate the irregular domain and the treatment of the boundary condition is complicated, while the unstructured grids present very good flexibility to the irregular domain and thus lead to more accurate results than that of structured grids for an irregular domain. The results of the proposed method are also compared with those calculated by FLUENT. Fig. 17 presents the comparison of the results calculated by the proposed method and FLUENT in cased 2 of Example 3. It is found that the result calculated by the proposed method agrees well with that calculated by FLUENT.

The three numerical examples demonstrated above indicate that the proposed unstructured grids-based discretization method for the convection–diffusion equations is reasonable and accurate.

4. Conclusions

This article proposes an unstructured grids-based discretization method for the convection–diffusion equations in cylindrical coordinates, in the framework of a finite volume approach. Numerical results have validated the correctness of the proposed method. Although, the proposed discretization method is performed only on unstructured triangular grids, it could be readily extended to that on an unstructured quadrilateral grids system. The study provides great convenience for the application of unstructured grids in a two-dimensional cylindrical coordinate system, leading to the flexibility of the discretization method for the irregular domains of any shapes.

Acknowledgements

The study is supported by National Key Projects of Fundamental R/D of China (973 Project: 2011CB610306) and National Science Foundation of China (Nos. 51134006, 51276198 and 51176204). This study is also supported by Science Foundation of China University of Petroleum, Beijing (No. 2462013YXBS009).

References

[1] M. Bilgili, Ö.E. Ataer, Numerical analysis of hydrogen absorption in a P/M metal bed, Powder Technol. 160 (2005) 141–148.
[2] R.D.C. Oliveski, A. Krenzinger, H.A. Vielmo, Comparison between models for the simulation of hot water storage tanks, Sol. Energy 75 (2003) 121–134.
[3] Y.-T. Yang, S.-Y. Tsai, Numerical study of transient conjugate heat transfer of a turbulent impinging jet, Int. J. Heat Mass Trans. 50 (2007) 799–807.
[4] R.D.C. Oliveski, M.H. Macagnan, J.B. Copetti, A.D.L.M. Petroll, Natural convection in a tank of oil: experimental validation of a numerical code with prescribed boundary condition, Exp. Therm. Fluid Sci. 29 (2005) 671–680.
[5] M. Sievers, U. Sievers, S.S. Mao, Thermal modelling of new Li-ion cell design modifications, Forsch. Ingenieurwes. 74 (2010) 215–231.
[6] W. Li, B. Yu, X. Wang, P. Wang, S. Sun, A finite volume method for cylindrical heat conduction problems based on local analytical solution, Int. J. Heat Mass Trans. 55 (2012) 5570–5582.
[7] C.W. Oosterlee, P. Wesseling, A. Segal, Benchmark solutions for the incompressible Navier-Stokes equations in general coordinates on staggered grids, Int. J. Numer. Methods Fluids 17 (1993) 301–321.
[8] G. Barakos, E. Mitsoulis, D. Assimacopoulos, Natural convection flow in a square cavity revisited: laminar and turbulence models with wall functions, Int. J. Numer. Methods 18 (1994) 677–695.